

# Sensing Global Changes in Local Patterns of Energy Consumption in Cities During the Early Stages of the COVID-19 Pandemic

Francisco Rowe (✉ [F.Rowe-Gonzalez@liverpool.ac.uk](mailto:F.Rowe-Gonzalez@liverpool.ac.uk))

Geographic Data Science Lab, Department of Geography and Planning, University of Liverpool  
<https://orcid.org/0000-0003-4137-0246>

Caitlin Robinson

Geographic Data Science Lab, Department of Geography and Planning, University of Liverpool

Nikos Patias

Geographic Data Science Lab, Department of Geography and Planning, University of Liverpool

---

## Research Article

**Keywords:** COVID-19, energy consumption, mobility, night-time light satellite imagery, cities

**Posted Date:** March 11th, 2022

**DOI:** <https://doi.org/10.21203/rs.3.rs-846222/v2>

**License:**  This work is licensed under a Creative Commons Attribution 4.0 International License.

[Read Full License](#)

---

# 1 Sensing Global Changes in Local Patterns of Energy 2 Consumption in Cities During the Early Stages of 3 the COVID-19 Pandemic

4 Francisco Rowe<sup>1,\*</sup>, Caitlin Robinson<sup>1</sup>, and Nikos Patias<sup>1</sup>

5 <sup>1</sup>Geographic Data Science Lab, Department of Geography and Planning, University of Liverpool, Liverpool, United  
6 Kingdom

## 7 ABSTRACT

COVID-19, and the wider social and economic impacts that a global pandemic entails, have led to unprecedented reductions in energy consumption globally. Whilst estimates of changes in energy consumption have emerged at the national scale, detailed sub-regional estimates to allow for global comparisons are less developed. Using night-time light satellite imagery from December 2019-June 2020 across 50 of the world's largest urban conurbations, we provide high resolution estimates (450m<sup>2</sup>) of spatio-temporal changes in urban energy consumption in response to COVID-19. Contextualising this imagery with modelling based on indicators of mobility, stringency of government response, and COVID-19 rates, we provide novel insights into the potential drivers of changes in urban energy consumption during a global pandemic. Our results highlight the diversity of changes in energy consumption between and within cities in response to COVID-19, moderating dominant narratives of a shift in energy demand away from dense urban areas. Further modelling highlights how the stringency of the government's response to COVID-19 is likely a defining factor in shaping resultant reductions in urban energy consumption.

# 9 1 Introduction

10 COVID-19, and the wider social and economic impacts that a global pandemic entails, have substantially reconfigured energy  
11 consumption patterns (Ruan et al., 2020), causing the biggest fall in global energy investment in history (International Energy  
12 Agency (IEA), 2020). With GDP shrinking by -3.3% globally during 2020 and recoveries diverging (International Monetary  
13 Fund (IMF), 2021), energy demand fell by -4% during 2020 compared to 2019 levels, impacting advanced economies most  
14 severely (IEA 2021). Global CO<sub>2</sub> emissions also fell by -5.8% during 2020 relative to 2019 (IEA 2020). Subsequently, Kanda  
15 and Kivimaa (2020) characterise COVID-19 as a ‘landscape shock’ during which rapid political action and emergency  
16 legislation - what energy transitions literature terms ‘disruptive policies’ (Geels et al., 2017) - have shaped the trajectory of  
17 energy transitions in unprecedented ways. Where previously government efforts to operationalise low carbon policies have  
18 been critiqued as slow and ineffectual, responses to COVID-19 have been characterised by suddenness and scale. Arguably  
19 cities have been central to these shifts (Batty, 2020; Connolly et al., 2020). However, there is evidence that many changes are  
20 temporary as CO<sub>2</sub> emissions returned to pre-pandemic levels during 2021 (Zheng et al., 2020).

21 The impact of COVID-19 on the wider energy system is an inherently geographical process, rearranging existing distri-  
22 butions, and scales, of socio-economic activity (Kuzemko et al., 2020). As such, like many aspects of the pandemic, energy  
23 consumption changes are socially, spatially and temporally uneven. During the early stages of the pandemic new energy  
24 consumption practices emerged as societies locked down to differing extents, energy-intensive industries were suspended and  
25 people spent a greater proportion of time at home. These patterns are especially stark in cities where energy and associated  
26 infrastructures are an integral part of life. In many contexts evidence has emerged of a subsequent shift in consumption from  
27 commercial, industrial and transportation energy sectors into the domestic sphere (Chen et al., 2020). Coupled with accelerated  
28 drops in energy prices (Norouzi et al., 2020), these reconfigurations have tested the finances and flexibility of electricity  
29 grids (Kanda and Kivimaa, 2020). Existing energy-related inequalities between and within countries have also been exacerbated  
30 as the negative impacts of the pandemic on finances and health have disproportionately impacted those who are already least  
31 sufficient in terms of domestic energy and mobility (Brosemer et al., 2020; Broto and Kirshner, 2020; Gebreslassie, 2020;  
32 Memmott et al., 2021).

33 To better understand the impact of COVID-19 on energy consumption, national-scale evidence has emerged (Bahmanyar  
34 et al., 2020; Gillingham et al., 2020; Ruan et al., 2020). However, changes in energy consumption are likely to be highly locally  
35 specific, varying according to socio-economic and urban structure, geographic context, and institutional or cultural change  
36 stimulated by COVID-19 (Kanda and Kivimaa, 2020). Subsequently, Acuto et al. (2020) make the case for “seeing COVID-19  
37 like a city” recognising the need to reach “beyond the confines of state-centric views to embrace the political-economic  
38 complexity of the ‘urban’” (p.978). In the absence of detailed administrative energy-related statistics, night-time light (NTL)  
39 satellite imagery can provide timely evidence of sub-regional changes in energy consumption during the pandemic (Beyer et al.,  
40 2021; Bustamante-Calabria et al., 2021; Green et al., 2021). NTL satellite imagery captures the intensity of visible lighting as  
41 observed from space. It can detect NTL emissions produced by artificial lighting in cities (e.g. buildings and transport hubs),  
42 moonlight and light reflected on the Earth’s surface (e.g. snow, water and vegetation) (Levin et al., 2020). While artificial city  
43 lighting encoded in NTL satellite imagery does not provide direct estimates of energy consumption, it can effectively capture  
44 changes in the spatial distribution of energy intensity over time. Hence, NTL satellite imagery data have been widely used  
45 for assessing electrification, detecting and monitoring power outages resulting from natural hazards, such as solar activity,  
46 earthquakes, winter storms, strong winds and tornadoes (Arribas-Bel et al., 2022; Min et al., 2013; Román et al., 2019; Wang  
47 et al., 2018), and can be an effective tool to capture changes in energy use during the COVID-19 pandemic (Green et al., 2021).

48 With this in mind, our analysis uses an urban lens to understand how patterns of energy consumption change in response  
49 to the pandemic via analysis of detailed NTL satellite imagery, focusing on 50 of the largest global cities. During the early  
50 stages of the pandemic, COVID-19 spread rapidly across the world via (inter)national linkages between major global cities,  
51 yet as the pandemic has progressed COVID-19 continues to circulate reaching deeper into rural and peri-urban areas with  
52 “planetary implications” (Acuto et al., 2020). Our analysis focuses on early stages of the pandemic, allowing us to evaluate  
53 how energy consumption in cities around the world changed in response to the pandemic as it first unfolded. We analyse NTL  
54 imagery from three months before and after 11th March 2020 (i.e. December 2019–June 2020), the date on which the World  
55 Health Organisation (WHO) declared COVID-19 a global pandemic. Although a global pandemic was not declared until March,  
56 city-scale lockdowns in some Chinese cities came into force in late January. Furthermore, in many countries around the world  
57 there was a significant lag between the timing of the first registered COVID cases and implementation of non-pharmaceutical  
58 interventions. By including imagery from January 2020 and February 2020 in our analysis (and comparing it with a December  
59 2019 baseline) we are able to capture a greater level of spatio-temporal variation in change. Our results therefore provide  
60 high-resolution estimates of spatiotemporal changes in urban energy consumption in response to COVID-19. To offer novel  
61 insights into potential drivers of changes in NTL intensity, we contextualise imagery with a range of sub-regional indicators of  
62 population density, COVID-19 cases and deaths, mobility estimates, and government response indicators. In doing so, the  
63 paper:

- 64 1. analyses city-scale changes in energy consumption in response to COVID-19;
- 65 2. identifies shifts in the spatial patterns of intra-urban energy consumption;
- 66 3. explores potential explanations for changes in urban energy consumption.

## 67 2 Materials and Methods

68 We analysed the patterns of energy consumption change in 50 of the largest global cities. A list of the cities is provided in the  
69 Supplementary Material (SM) Table 1. Three reasons underpin our selection of cities. First, with the exception of Milan (Italy)  
70 (included as an epicentre of the initial COVID-19 outbreak), all cities rank within the top 110 largest urban agglomerations  
71 based on population size, with over 4.2 million estimated inhabitants in 2020 (United Nations, 2018), to ensure some level of  
72 consistency comparing cities of equivalent size. Second, we sought to provide a diverse geographically perspective. Cities were  
73 selected to represent a diversity of national contexts across the Global North and Global South. In countries with a number of  
74 large cities we typically selected a single representative city to ensure that as diverse a national sample was selected as possible.  
75 Third, we also sought to identify the similarity and differences in the effects of COVID-19 on urban energy use globally. City  
76 extents were defined using Functional Urban Area (FUA) boundaries which provide a consistent classification based on density  
77 and commuting flows (Schiavina et al., 2019). Our analytical framework consists of four main stages. Each of these stages is in  
78 turn described below.

79 We adopted an open and reproducible research approach based on the use of open software for satellite imagery and  
80 statistical analysis - see Code Availability Section. As indicated below, all data were obtained from publicly available sources  
81 and organised in the form of an open data package - see Data Availability Section. We followed best practices in geographic  
82 data science (Brunsdon and Comber, 2021) and produce an open data product (Arribas-Bel et al., 2021), including software  
83 code to reproduce or extend our analysis, which is available for download as indicated in the Code Availability Section.

### 84 2.1 Night-time light (NTL) imagery analysis

85 To understand changes in energy consumption in response to the pandemic in each city, we analyse NTL satellite imagery. NTL  
86 imagery captures daily and detailed nocturnal visible light observations of the Earth, providing a unique source to monitor  
87 the spatial distribution and intensity variations of human activity at local and planetary scales in near-real time. In addition  
88 to street lighting, NTL satellite imagery captures any type of visible light emanating from residential buildings, vehicles, car  
89 parks, offices, factories and illuminated sporting venues. NTL data have extensively been used to study electricity consumption,  
90 socio-economic activities, light pollution, urban extent changes and power outages (Levin et al., 2020). In the context of  
91 COVID-19, NTL imagery has been used to understand the initial impact on the US electricity sector (Ruan et al., 2020), changes  
92 in CO<sub>2</sub> emissions nationally (Zheng et al., 2020), changes in economic activity in the core of global megacities (Xu et al.,  
93 2021) and changes in energy use during the COVID-19 pandemic in specific Brazilian (Carvalho et al., 2021) and European  
94 cities (Werth et al., 2021).

95 We used a monthly composite of NTL data produced by the Payne Institute for Public Policy under the Colorado School of  
96 Mines (<https://payneinstitute.mines.edu/eog/nighttime-lights/>). We utilised the version 1 monthly  
97 series of global average radiance composite images from the Visible Infrared Imaging Radiometer Suite (VIIRS) Day-Night  
98 Band (DNB) sensor on the Suomi National Polar-orbiting Partnership satellite. The DNB encodes records of visible near-  
99 infrared NTL intensity which is measured in radiance units i.e. nanoWatts/cm<sup>2</sup>/sr ( $nWcm^{-2}sr^{-1}$ ). The spatial resolution of  
100 VIIRS data is 15 arc-seconds (450m) across the latitudinal zone of 65°S-75°N5, providing global coverage with 12hr revisit  
101 time (Cao et al., 2017) and a local overpass time of 01:30am (Elvidge et al., 2013). The data version used in our study is the  
102 monthly VIIRS Cloud Mask product. These data are corrected for stray light as well as the effects of biogeophysical processes,  
103 such as seasonal vegetation and snow (Miller et al., 2013). The data are however not corrected for temporal lights, including  
104 fires and boats. Following Li et al. (2020), we used an empirical threshold of 0.3  $nWcm^{-2}sr^{-1}$  to remove dim light noises  
105 caused by these forms of temporal lights. The threshold was subtracted from the VIIRS image and negative pixel values were  
106 set to zero. This noise removal operation was conducted using Google Earth Engine. For our analysis, we used cloud free data,  
107 and assessed if zero values in the average radiance imagery for our sample of cities effectively encoded no lights, as regions  
108 towards the poles during summer months have no data due to solar illumination. As a result, imagery for six time points was  
109 excluded from the analysis (SM Figure 1).

110 The result from these steps are a series of monthly global composites for between December 2019 and June 2020 (Figure 1).  
111 Each pixel within the image represents an area of 450m<sup>2</sup>. In analysing changes in NTL intensity, it is necessary to assume that  
112 these changes are the result of COVID-19 and associated restrictions; however, we acknowledge that other factors could have  
113 contributed (e.g. national holidays, blackouts and seasonal variations). As a result, as explained below, we further contextualise  
114 the imagery with additional indicator data sets: daily national estimates of stringency of government response (Hale et al., 2021);

115 population density estimates (Stevens et al., 2015); confirmed COVID-19 cases (Ritchie et al., 2020); and daily sub-regional  
116 mobility estimates (Google, 2020).

## 117 2.2 Measuring city-scale changes in night-time lighting

118 To measure the overall extent of changes in energy consumption patterns in cities, we computed three summary indicators. All  
119 three indicators are based on the difference between the radiance for individual months and for December (our baseline). The  
120 first indicator is the mean number of pixels (Equation 1). It indicates the number of pixels defining individual cities that recorded  
121 a change on average across pixel differences for individual months ( $m_t$ ) and the baseline month ( $m_0$ ) (i.e. December, 2019).  
122 Averages were computed conditionally for pixels indicating negative, neutral and positive change ( $C$ ). The second indicator  
123 is the average percentage of pixels in each category: negative, neutral and positive (Equation 2). This indicator accounts for  
124 variations in city size to enable comparisons across cities. The third indicator is the median radiance ( $r$ ) of night-time intensity  
125 across the difference from the baseline for each of the six months. This indicator provides an estimate of the total change in  
126 NTL intensity in individual cities, as well as the overall direction of this change (i.e. positive and negative). For this indicator  
127 we reported only two categories (i.e. positive and negative), as the median for the neutral category is zero. In addition to these  
128 indicators, we analysed the full distribution of the difference in NTL radiance between individual months and December, 2019.  
129 Given small numbers, extreme NTL scores (i.e. above 30) are set to 30.

$$n = \frac{\sum_{t=1, m \in C}^6 m_t(C) - m_0(C)}{6} \quad (1)$$

$$p = \frac{\sum_{t=1, m \in C}^6 \frac{m_t(C) - m_0(C)}{m_t - m_0}}{6} \quad (2)$$

$$n = \frac{\sum_{t=1, m \in C}^6 \text{median}[r_t(C) - r_0(C)]}{6} \quad (3)$$

130 To define city extents, we used a set of Functional Urban Area (FUA) boundaries developed in a collaborative project between  
131 the Organisation for Economic Co-operation and Development and the Global Human Settlement layer project (Schiavina et al.,  
132 2019). Delimiting the extent of cities is challenging, and the FUA boundaries overcome this problem providing a consistent  
133 way to define extents based on population density measured at a fine spatial resolution ( $1km^2$  grids). First, adjacent grids of  
134 high density are clustered together. Then the level of commuting flows is measured to integrate non-continuous areas that  
135 display a distinctive urban centre of employment.

## 136 2.3 Analysing intra-urban changes in night-time lighting

137 To understand intra-urban changes, we conducted two sets of analyses. First, we examined the association between population  
138 density and NTL intensity using Generalised Additive Models (GAMs). We sought to assess if more densely populated areas in  
139 cities experienced larger average declines in NTL intensity, arguably reflecting the location of employment centres. To this end,  
140 population density data were obtained from the WorldPop project (<https://www.worldpop.org>). These data comprise a  
141 raster layer covering the entire world and provide population density estimates at  $1km^2$  grids. The data set is based on the United  
142 Nations' population count data using a top-down methodological approach (Stevens et al., 2015). In this approach, population  
143 counts at administrative units level are disaggregated to grid-cell based counts by using a series of detailed geospatial data sets,  
144 such as land cover, night-time imagery and proximity to amenities as covariates in a random forest estimation framework.

145 In a second analysis, we assessed the spatial distribution of NTL change between January and June, 2020. We mapped  
146 the changes in NTL intensity for individual cities, and classified them based on the spatial structure of these changes during  
147 the month local lockdowns were enacted, or the following month if lockdowns were introduced towards the end of a month  
148 (SM Table 2 provides a list of start dates of local lockdowns for each city). We categorised cities into three classes: whole  
149 city, fragmented and spatially concentrated patterns of change. Whole city change encompasses cities displaying widespread  
150 dimmed or brightened patterns of NTL intensity. Fragmented change includes cities displaying scattered patterns of change.  
151 Spatially concentrated involves cities displaying geographically focused patterns of change. We observed three distinctive  
152 patterns: (1) changes along network infrastructures; (2) a core-periphery configuration; and, (3) systematic localised changes in  
153 key areas of cities.

## 2.4 Modelling mobility, stringency and COVID-19 infection

We also sought to understand the temporal patterns of urban energy use, non-pharmaceutical interventions and COVID-19 incidence. We used a hierarchical two-level modelling approach to capture time-city level interactions at level 1 and city-specific patterns at level 2. Monthly NTL data afford very limited temporal granularity, so we used Google Mobility Report data to capture these dynamics. The percentage change in stay-at-home population was used as a proxy for shifts in urban energy use. We argue that this is a reasonable proxy as we expect that increases in stay-at-home population and simultaneous drops in time spent at work over time would lead to be associated with changes in the patterns of urban energy use. Analysis of Google workplace and residential mobility data reveals that increases in stay-at-home population mirror declines in time spent at work (SM Figure 4).

We estimated a series of hierarchical regression models using the percentage change of stay-at-home population as a function of a stringency indicator and COVID-19 incidence in a generalised linear mixed model (GLMM) framework. Intuitively, all estimated models included a stringency indicator and COVID-19 incidence measured at time  $t$ , and a stringency indicator at time  $t - 1$  recognising the delayed effects of lockdowns on influencing mobility patterns. For interpretation and identification purposes, independent variables were standardised, subtracting the mean and dividing by the standard deviation. We used natural splines to account for systematic temporal variations in the data, and incorporated natural splines as overall and city-specific parameters. We also included a temporal autoregressive term to account for temporal dependency. We evaluated the inclusion of temporal lags of higher order for the stringency indicator and COVID-19 incidence. Correlation coefficients and estimates for these variables are very small in size and statistical significance. We report a correlation matrix and two models in the SM Table 3 and Figure 5 providing evidence for this.

More formally, we present evidence from three different model specifications in the manuscript (Figure 5). These models are mathematically formulated in Equations 4-6:  $y_{it}$  captures change in stay-at-home population at city  $i$  in time  $t$ ;  $\beta_{0i}$  is the random intercept that varies across cities;  $\beta_{1i}$  is the slope of the associated stringency indicator  $s_{it}$ ;  $\beta_{2i}$  is the slope of the lagged stringency indicator at  $t - 1$ ;  $\beta_{3i}$  is the slope of new COVID-19 cases  $c_{it}$ ;  $\sum_{k=1}^{n+1} \beta_{ki} B_{kit}$  represents random natural spline slopes at three knot points that vary across cities and capture systematic temporal patterns in stay-at-home population changes (see [Hastie et al. \(2009\)](#) for details on splines);  $\varepsilon_{it}$  is the city-time-level residual term that is assumed to be of first-order autoregressive ( $\Omega_\varepsilon$ ); that is, residuals are assumed to be correlated. Residuals at time  $t - 1$  are assumed to influence residuals at time  $t$ . Equations relating to  $\beta_{0i}$  and  $\beta_{ki}$  correspond to the random effects, or city-varying intercept and natural spline slopes, respectively. They capture variations in the associated parameters across cities and have unexplained heterogeneity denoted by  $u_{0i}$  and  $u_{ki}$ . These error terms follow an independent normal distribution  $N(0, \sigma_{u_0}^2)$  and  $N(0, \sigma_{u_1}^2)$ .

$$\begin{aligned}
 y_{it} &= \beta_{0i} + \beta_{1i}s_{it} + \beta_{2i}s_{it-1} + \beta_{3i}c_{it} + \sum_{k=1}^{n+1} \beta_{ki}B_{kit} + \varepsilon_{it} \\
 \beta_{0i} &= \beta_0 + u_{0i} \\
 \beta_{ki} &= \beta_k + u_{ki} \\
 \varepsilon_{it} &\sim N(0, \Omega_\varepsilon)
 \end{aligned}
 \tag{4}$$

The key difference across Equations 4-6 is in the parameter allowed to vary across cities. In Equation 4, natural spline parameters are allowed to vary across cities capturing differences of systematic temporal fluctuations in stay-at-home population. We report the estimates for  $\beta_{1i}$ ,  $\beta_{2i}$  and  $\beta_{3i}$  from this model as it provides the smallest Akaike Information Criterion (AIC) score. Though coefficients across all three models are fairly consistent in size. In Equation 5,  $\beta_{1i}$  is allowed to vary across cities. This coefficient captures differences in the association between changes in stay-at-home population and the stringency indicator. In Equation 6,  $\beta_{3i}$  is allowed to vary across cities. This coefficient captures differences in the association between changes in stay-at-home population and new COVID-19 cases. In addition, Equation 6 also includes a lagged term ( $\beta_{4i}$ ) for new COVID-19 cases to capture the lagging effect in the relationship between changes in stay-at-home population and new COVID-19 cases. All models included natural spline parameters in the fixed part of the model and a first-order autoregressive error term was assumed for the city-time level residuals.

$$\begin{aligned}
 y_{it} &= \beta_{0i} + \beta_{1i}s_{it} + \beta_{2i}s_{it-1} + \beta_{3i}c_{it} + \sum_{k=1}^{n+1} \beta_{ki}B_{kit} + \varepsilon_{it} \\
 \beta_{0i} &= \beta_0 + u_{0i} \\
 \beta_{1i} &= \beta_1 + u_{1i} \\
 \varepsilon_{it} &\sim N(0, \Omega_\varepsilon)
 \end{aligned}
 \tag{5}$$

$$y_{it} = \beta_{0i} + \beta_{1i}s_{it} + \beta_{2i}s_{it-1} + \beta_{3i}c_{it} + \beta_{4i}c_{it-1} + \sum_{k=1}^{n+1} \beta_{ki}B_{kit} + \varepsilon_{it} \quad (6)$$

$$\beta_{0i} = \beta_0 + u_{0i}$$

$$\beta_{3i} = \beta_3 + u_{3i}$$

$$\varepsilon_{it} \sim N(0, \Omega_\varepsilon)$$

*Google Mobility Data:* In response to COVID-19, Google released Community Mobility Reports to help inform public health responses to COVID-19 (<https://www.google.com/covid19/mobility/>). The data set measures the change in the number of visitors (or time spent) in relation to a baseline period. The baseline corresponds to the median value from the 5-week period January 3-February 6, 2020. The changes are categorised according to specific places or sectors: retail and recreation; groceries and pharmacies; parks; transit stations; workplaces; and residential. We focused our analysis on the residential category which indicates the change in stay-at-home population.

*Stringency index:* We used a stringency index to capture the level and variation of non-pharmaceutical interventions (<https://covidtracker.bsg.ox.ac.uk>). The stringency index is a composite indicator based on nine response indicators: school closures; workplace closures; cancellation of public events; restrictions on gatherings; public transport restrictions; public information campaigns; and stay at home measures (Hale et al., 2021). The index, available since 1st January 2020, computes a simple score by adding together the nine indicators which is rescaled to vary between 0 and 100. The stringency index is intended for comparative purposes, rather than as an indicator of how effective national policies have been at tackling the spread of COVID-19 (Hale et al., 2021).

*COVID-19 cases:* Data on the number of COVID-19 cases were obtained from Our World in Data (Ritchie et al., 2020). We also analysed the relationship between COVID-19 deaths and changes in stay-at-home population. We do not report these analyses in the main manuscript as we argue that COVID-19 cases were a more prominent measure of public knowledge in the early stages of the pandemic. We believe that individual responses during this period were more a result of the extent and rate of spread of COVID-19, rather than the actual number of deaths. We do however report analysis on COVID-19 in the SM Figure 3 and 4.

## 3 Results and discussion

### 3.1 City-scale changes in energy consumption patterns during COVID-19

Comparison of imagery from December 2019 and each month between January 2020 and June 2020 yields three city-scale summary indicators of average NTL intensity (see Methods and Supplementary Materials (SM) Table 1), each a proxy for changes in urban energy consumption (Figure 2). Firstly, the mean number of pixels indicator (left) indicates the proportion of pixels in each city for which the average change was either negative, neutral or positive. To account for variation in city size (with indicators based on number of pixels likely prioritising larger, less dense urban conurbations), a second indicator is provided based on the mean percentage of pixels (centre). Thirdly, an indicator of median percentage change illustrates the strength of change in NTL intensity (positive or negative). Based on the summary indicators, there is considerable variation in changes in energy consumption between selected cities.

Based on the mean percentage of pixels, in selected cities a high proportion of pixels experienced no change in NTL intensity during the six month period. In four cities this represented over half of pixels: Manila (53%) Osaka (60%), Melbourne (69%) and Dhaka (74%). Elsewhere, the mean percentage of pixels was overwhelmingly negative: Shanghai (56%), Beijing (51%); Johannesburg (54%), Luanda (53%), and Milan (54%). For several cities, particularly in the Middle East, change was largely positive, including Tehran (50%), Moscow (55%) and Baghdad (64%). The strength of change also varies as reflected by the median percentage change indicator. In Lima there was a large difference between the median negative (-25%) and positive percentage change (+ 22.75%) indicating considerable diversity in NTL intensity across space and time.

For other cities, the distribution of change in pixels is relatively similar for each time period (e.g. Melbourne; Osaka; Manila) (Figure 3) suggesting that the spatial distribution of NTL intensity is relatively stable over time. In Melbourne little change was experienced over time, likely reflective of stringent border closures that have enabled a national zero-COVID strategy (Phillips, 2021). In other cities, where there was greater variation in the distribution of change (e.g. Karachi, Tehran, Kinshasa, Mumbai) detailed examination of the intra-urban distribution of NTL intensity is useful.

### 3.2 Shifting spatial patterns of intra-urban energy consumption during COVID-19

Examination of the relationship between population density and NTL intensity (Figure 4) provides insight into the intra-urban distribution of energy consumption in response to COVID-19. Much attention has been paid to the risk of infection in dense

237 urban centres (Hamidi et al., 2020; Xu et al., 2021), particularly during the early stages of the outbreak. This is evident in cities  
238 in which NTL intensity declined in densely populated areas (e.g. Johannesburg; Karachi; Kinshasa; Tokyo; Toronto). However,  
239 for the majority of cities we observe little association between the variables, with some cities experiencing a relative increase in  
240 light intensity in densely populated areas (e.g. Delhi, Melbourne; Rio de Janeiro; New York).

241 From closer inspection of mapped NTL intensity (for imagery for all 50 cities see SM Figure 2), three distinctive spatial  
242 configurations in energy use are identified: (i) whole city; (ii) fragmented; and (iii) spatially concentrated (Figure 5). This  
243 classification is not exhaustive, rather it illustrates the type, consistency and diversity of change in cities globally in response to  
244 COVID-19.

245 Firstly, selected cities experience a whole city change in NTL intensity. In Beijing, where a national lockdown was  
246 implemented in February, dimming of the majority of the pixels occurred (see also Addis Ababa; Beijing; Buenos Aires; Cairo;  
247 Luanda; Mexico City; Rio de Janeiro; São Paulo; Santiago; Shanghai; Toronto; Wuhan). Comparatively, in a small number of  
248 cities including Dar es Salaam, the majority of pixels brightened (see also Abidjan; Baghdad and Kabul). Secondly, selected  
249 cities experienced fragmented changes with pixels increasing and decreasing across the city with limited spatial patterning.  
250 This was the case in Los Angeles and Singapore when lockdown restrictions were introduced in March (see also Istanbul;  
251 Johannesburg; Kuala Lumpur; London; Melbourne; Milan; New York; Osaka; Rome; Singapore; Tokyo). Thirdly, spatially  
252 concentrated changes in NTL intensity also occurred. Spatially concentrated changes were wide-ranging, reflecting diverse  
253 urban structures. Changes in some cities were shaped by networked infrastructures illustrative of connectivity (i.e. based on  
254 roads and economic corridors) that arguably play an integral role in the spread of COVID-19 (Hamidi et al., 2020). In Delhi,  
255 networked infrastructures dimmed in March in response to restrictions (see also Bangkok and Lahore), whilst in Moscow  
256 infrastructures brightened. Elsewhere, spatially concentrated forms of change replicated classic core-versus-periphery structures  
257 of cities (Dhaka; Karachi; Lagos; Madrid; Manila; Mumbai; Paris; Riyadh; Seoul; Tehran; Yangon). Yet in Lima, during March  
258 when lockdown was implemented, the core of the city brightened whilst the periphery dimmed. For some cities, hot spots of  
259 both dimming and brightening emerged (Bogota, Ho Chi Minh City; Hong Kong; Jakarta; Kinshasa Nairobi).

260 Where a whole city scale or spatially concentrated dimming of a city occurred, this is indicative of a variety of socio-spatial  
261 trends in response to COVID-19. Previous research on energy use and COVID-19 has evidenced substantial reductions in  
262 areas of concentrated economic activity. For example, there is evidence of heightened reductions in electricity consumption in  
263 areas with a high level of commercial activity (Ruan et al., 2020). As non-essential businesses close, schools and workplaces  
264 transition online and strict travel restrictions are implemented, evidence has also emerged of a transfer of energy consumption  
265 into the domestic sphere. For example, Liu et al. (2020) evidence increased activity in residential areas, decreased activities  
266 in commercial centres, and similar activity levels in transport and public facilities. In some cities a proportion of affluent or  
267 transient urban residents, no longer tied to places of employment, temporarily migrated away from dense urban areas where the  
268 perceived risks of contracting the virus are most acute (Connolly et al., 2020), thus contributing towards a suburbanisation of  
269 energy consumption. For example, in Wuhan where the virus first emerged, an estimated five million residents left the city prior  
270 to lockdown (Pinghui and Ma, 2020).

271 Further detailed analysis of cities with a spatially concentrated change offers insight into how NTL intensity is shaped by  
272 the degree and type of industrialisation in a city. Many highly industrialised areas - including energy intensive industrial zones  
273 and infrastructural corridors typically associated with high NTL intensity - experienced a concentrated reduction in energy  
274 consumption, as non-essential manufacturing halted during the pandemic. For example, in Wuhan, energy intensity reduced  
275 dramatically in the Optics Valley of China, the largest producer of fiber optic cable in the world, and the Wuhan subsidiary of  
276 the China Baowu Steel Corporation, one of the foremost global steel producers. Dimming of major energy infrastructures is  
277 also apparent, reflecting the role of global energy systems and markets in shaping urban energy intensity. For example, Riyadh  
278 Oil Refinery part of Saudi Aramco - a company with the world's second-largest proven crude oil reserves - dimmed as demand  
279 for oil hit a 25 year low in response to COVID-19 (Ambrose, 2020).

280 Yet as evidenced in the NTL imagery, some cities contradict more commonly documented trends of a reduction or  
281 suburbanisation of energy consumption. For example, in Dar es Salaam (a city that brightened overall) restrictions on socio-  
282 economic activities were relatively light-touch attributed to the political response to the pandemic (Makoni, 2021), coupled  
283 with concerns about impacts of lockdown on employment (Mfinanga et al., 2021). In selected cities, patterns also changed  
284 considerably over time. For example, in Lima one of the regions worst hit by COVID-19 (Munayco et al., 2020), a brightening  
285 of the core and dimming of the periphery from February until April gave way to a complete dimming in May and June.

### 286 3.3 Explaining changes in urban energy use through changes in mobility, stringency of government re- 287 strictions and COVID-19 incidence

288 The diversity of configurations evidenced over both space and time suggests that multiple factors shape changes in urban energy  
289 consumption in response to COVID-19. We examine the association between temporal shifts in energy use patterns, and changes  
290 in COVID-19 incidence and non-pharmaceutical measures. We recognise the distinctive dynamics of this association across

291 cities by employing a hierarchical two-level modelling approach, at level 1 capturing time-city interactions and level 2 capturing  
292 city-specific patterns (see Methods Section). Monthly NTL imagery affords limited temporal granularity, so we used Google  
293 Mobility Report data to capture these dynamics. Changes in mobility, specifically in the share of stay-at-home population,  
294 serve as a proxy for shifts in urban energy use (Mohammadi and Taylor, 2017). To measure non-pharmaceutical interventions,  
295 we used a stringency index which is a composite indicator that measures the extent and variation of non-pharmaceutical  
296 interventions globally, ranging from 0 (no measures) to 100 (the strictest scenario) (Hale et al., 2021).

297 We recognise two important features in the association between these factors. First, the relationship between changes in  
298 mobility (energy use), COVID-19 incidence and non-pharmaceutical measures represents multiple causal mechanisms, arising  
299 from “top-down” government interventions and “bottom-up” individual responses. For instance, strict non-pharmaceutical  
300 measures may result in business and school closures, reducing mobility, increasing the share of stay-at-home population and  
301 ultimately domestic energy consumption. Conversely, rising COVID-19 case transmission, particularly early in the pandemic,  
302 may have led to increasing public concern fuelled by anxiety and fear with a rising number of stay-at-home population and  
303 domestic energy usage as a result of reduced workplace activity.

304 Second, these relationships exhibit different temporal dynamics across cities (Figure 6a and 6b). Certain cities (Mel-  
305 bourne, Kuala Lumpur, Delhi, Manila, Lagos) display large increases in stay-at-home population associated with strict  
306 non-pharmaceutical interventions despite relatively small rises in COVID-19 cases. Cities like Singapore, Paris, Madrid,  
307 Santiago and Lima show equally large increases in stay-at-home population and strict interventions; yet report consistently high  
308 numbers of COVID-19 cases. Others, including Bangkok and Seoul, display moderate increases in stay-at-home population  
309 despite strict non-pharmaceutical interventions.

310 Figure 6c-e reports our modelling of changes in the share of stay-at-home population as a function of stringency intervention  
311 and new COVID-19 cases (see Methods and SM Table 3 for full model estimates). Main fixed effects are displayed in Figure  
312 6c, and random, varying city slopes for stringency and new COVID-19 cases in Figures 6d-6e, respectively. Compared to  
313 COVID-19 cases, a larger and positive estimate for local stringency measures ( $\beta = 4.69$ ; 95%  $CI = 3.85 - 5.52$ ) (Figure 6c)  
314 suggests that the enactment of “top-down” stringent lockdown played a major role in incentivising working from home and  
315 hence domestic energy consumption across most cities in our sample. Coupled with a positive but smaller estimate for local  
316 stringency at time t-1 ( $\beta = 2.73$ ; 95%  $CI = 2.02 - 3.45$ ), these findings also suggest that the largest impact of stringency  
317 measures on reducing travel-to-work activity was immediate but it takes some time for this to be fully realised.

318 Figure 6d-6e reveals the extent of variation in the association between changes in the share of stay-at-home population, and  
319 stringency measures and new COVID-19 cases across our sample of cities. Cross-tabulating estimates for these associations,  
320 we identify four groupings of cities (Figure 6f):

- 321 • Group one includes cities with greater than average stringency and COVID-19 cases estimates, (e.g. Kuala Lumpur,  
322 Manila and Mumbai). Underpinning these results are relatively high shares of stay-at-home population (40%) and  
323 arguably domestic energy use, coupled with high levels of stringency (100) and continuously small numbers of COVID-19  
324 cases (<15 per million) (Figure 6a-b).
- 325 • Group two display larger than average stringency but lower COVID-19 cases estimates (e.g. Lagos, Bogota, Lima and  
326 Johannesburg). This reflects initially large and subsequently moderate increases in stay-at-home population (ranging  
327 from 40%-20%) and domestic energy use, and moderate rises in COVID-19 cases despite strict lockdown interventions  
328 early in the pandemic (i.e. March) (Figure 6a-b and SM Table 3).
- 329 • Group three includes cities with smaller than average stringency and COVID-19 case estimates (e.g. Bangkok, Osaka,  
330 Cairo, Moscow and New York). These cities display moderate rises in the share of stay-at-home population (<25%) and  
331 domestic energy use despite stringent measures, with varying outcomes of COVID-19 cases: persistently low in Bangkok,  
332 Osaka and Cairo, and relatively high in Moscow and New York.
- 333 • Group four comprises a small set of cities displaying small stringency but greater than average COVID-19 cases estimates  
334 (e.g. Seoul and Tokyo). These patterns reflect a trend of moderate stay-at-home population shares (<20%), low COVID-19  
335 cases and stringency measures. In South Korea, transmission was controlled by employing less stringent social distancing  
336 measures than in Europe and the United States (Watanabe and Yabu, 2021). Similarly, Japan did not impose stringent  
337 lockdown measures, but enacted a state of emergency strategy to encourage people to stay at home (Dighe et al., 2020).

338 These overarching trends suggest that “top-down” emergency restrictions and legislation introduced by national governments  
339 have played a substantial role in reconfiguring social and economic structures, and therefore energy consumption patterns, in  
340 the majority of cities selected. However, where government response has been relatively light touch, “bottom-up” changes in  
341 energy-related practices owing to the response of individuals or employers to the crisis assume greater importance in shaping  
342 energy consumption (Schot et al., 2016). In the absence of emergency legislation, people are still required to engage in essential

343 everyday activities that encourage energy consumption e.g. commuting. However, our results show that energy consumption  
344 and mobility declined moderately over time, as non-essential energy-related activities were foregone in response to the increased  
345 incidence of COVID-19.

## 346 **4 Conclusions**

347 Energy production, demand consumption is highly locally contingent and spatially uneven (Baka and Vaishnava, 2020;  
348 Broto and Baker, 2018). Analysis of socio-spatial datasets can provide unique insights into the geographical distribution  
349 of energy consumption at a range of scales (Bouzarovski and Thomson, 2018; Robinson et al., 2019). In our analysis of  
350 energy consumption during COVID-19 using NTL imagery, whilst global, and typically national, demand for energy fell  
351 overall in response to COVID-19 and accompanying restrictions (especially in contexts where per-capita energy use is typically  
352 high) (IEA, 2021) new spatial distributions have emerged between and within cities.

353 Our analysis provides a first global assessment of the city-scale changes in energy consumption patterns during COVID-19,  
354 evidencing considerable variations in changes across the largest 50 urban agglomerations in the world. For some cities, changes  
355 in energy consumption as indicated by NTL intensity are overwhelming negative in response to COVID-19, yet elsewhere  
356 the reverse pattern is observed. We also provided evidence of five distinctive signatures of changes in the spatial patterns  
357 of intra-urban energy consumption within cities, reflecting widespread and more localised geographical changes across the  
358 urban landscape. This evidence expands existing predominant narratives suggesting the “suburbanisation” of energy demand in  
359 several urban contexts during the early phases of COVID-19 as the dominant spatial pattern of energy usage as lockdowns were  
360 enacted, business and services were closed, and home working became the predominant form of employment (Abdeen et al.,  
361 2021; Krarti and Aldubyan, 2021; Qarnain et al., 2020). We provided evidence that suburbanisation is one of five distinctive  
362 ways in which energy consumption has been reconfigured within large cities across the globe.

363 We also presented statistical evidence suggesting that, while variability exists, government stringency responses to mitigate  
364 the spread of COVID-19 were a key factor in shaping changes and reductions in urban energy consumption observed in most  
365 cities in our sample during the early stages of the pandemic. Equally, individual behavioural responses to minimise exposure to  
366 COVID-19 also appeared to have resulted in higher local shares of stay-at-home population and hence declines in urban energy  
367 consumption in cities, but to a lesser extent. Taken together, these findings suggest that structural policy responses are key to  
368 generate large-scale changes in energy use, and support the need for ambitious national and global policies that substantially  
369 reconfigure social and economic systems, rather than individual behaviour change - if the necessary scale of change for a  
370 low-carbon society is to be achieved. Our study thus contributes to the ongoing debate about whether COVID-19 is likely to act  
371 as a catalyst for a permanent reduction in urban energy consumption owing to digitalisation of work and other activities (Kanda  
372 and Kivimaa, 2020), and indeed as inspiration for transitions to a low carbon society (Henry et al., 2020).

373 Our analysis analyses changes in the spatial patterns of urban energy use during night-time as encoded in NTL satellite  
374 imagery based on lighting from urban features and mobility. Overall domestic energy consumption increased during the  
375 pandemic; the most significant change is in the shape of the load profiles during the day time as household schedules and  
376 day-time mobility patterns change. Further research is thus needed to capture these shifts in demand for energy during the  
377 day and understand the energy-related household practices or industrial energy usage underpinning these changes as estimates  
378 of energy consumption become available. Our analysis focuses on large global urban conurbations. Understanding changes  
379 in energy patterns in smaller cities or rural and peri-urban areas is also important as these areas recorded a large influx of  
380 population moving away from large density areas, suggesting a transfer of energy demand from urban agglomerations to smaller  
381 areas (González-Leonardo et al., 2022; Rowe et al., 2022).

382 Additionally, our analysis captures changes in the spatial distribution of urban energy during COVID-19. While these  
383 changes may largely reflect, as we believe, the effects of lockdowns, they may also reflect seasonal variations in the distribution  
384 of population across cities as some parts of the world transitioned from winter into spring. More importantly, identifying the  
385 causes of changes in energy consumption observed in large cities over the early stages of the pandemic and extending the  
386 period of analysis could be key to better understand the extent to which the changes brought about by COVID-19 are temporary  
387 or will endure as hybrid working becomes ingrained in societies. Evidence of changes in energy consumption post-lockdown  
388 suggests that recovery to pre-lockdown levels is socially and spatially uneven, with relatively affluent areas experiencing a  
389 rapid recovery compared to poorer regions (Aruga et al., 2020; Zheng et al., 2020). Detailed spatial analyses of NTL imagery  
390 beyond June 2020 could provide insight into the longer-term impacts of COVID-19, including inequalities embedded in the  
391 recovery of energy consumption levels post-lockdown.

## 392 **Data availability**

393 The data used for our analysis is publicly available online: monthly VIIRS NTL satellite imagery composites (version 1) from  
394 the Earth Observations Group (EOG) Payne Institute for Public Policy, [https://eogdata.mines.edu/download\\_](https://eogdata.mines.edu/download_)

395 [dnb\\_composites.html](#); daily COVID-19 pandemic data from Our World in Data, [https://github.com/owid/](https://github.com/owid/covid-19-data/tree/master/public/data)  
396 [covid-19-data/tree/master/public/data](#); social distancing and lockdown data from the Oxford COVID-19  
397 Government Response Tracker (OxCGRT), <https://github.com/OxCGRT/covid-policy-tracker>; Google mobility  
398 data, <https://www.google.com/covid19/mobility/>; and, global population data from the WorldPop project,  
399 <https://www.worldpop.org/project/categories?id=18>. The results supporting the findings of this study are  
400 provided in the main text and Supplementary Information. The source data underlying all the figures in the main manuscript  
401 and Supplementary Information are provided as a Source Data file. Source data to replicate the results reported in the paper  
402 are provided in an Open Science Framework (OSF) repository, DOI: [xxx] (<https://xxx>), except for the monthly VIIRS NTL  
403 imagery composites which exceed the data storage capacity in Github. VIIRS NTL composites can be obtained from the first  
404 link provided in this paragraph.

## 405 Code availability

406 The code to reproduce all the analysis and figures reported in this study are openly available in an Open Science Framework  
407 (OSF) repository, DOI: [xxx] (<https://xxx>). The analysis was performed in RStudio 1.3.959 running on R version 4.0.2 (2020-  
408 06-22) using the following list of packages sorted in alphabetical order: “countrycode 1.2.0”, “corrplot 0.84”, “glimmTMB  
409 1.0.2.1”, “ggpubr 0.4.0”, “grid 4.0.2”, “gridExtra 2.3”, “lubridate 1.7.9”, “osmdata 0.1.3”, “raster 3.3-13”, “rvest 0.3.6”, “sf  
410 0.9-5”, “tmtools 3.1”, “tidyverse 1.3.0”, “viridis 0.5.1”. Refer to the README in the repository for instructions.

## 411 References

- 412 Abdeen, A., Kharvari, F., O’Brien, W., and Gunay, B. (2021). The impact of the COVID-19 on households’ hourly electricity  
413 consumption in Canada. *Energy and Buildings*, 250:111280. [https://doi.org/10.1016/j.enbuild.2021.](https://doi.org/10.1016/j.enbuild.2021.111280)  
414 [111280](#).
- 415 Acuto, M., Larcom, S., Keil, R., Ghojeh, M., Lindsay, T., Camponeschi, C., and Parnell, S. (2020). Seeing COVID-19 through  
416 an urban lens. *Nature Sustainability*, 3:977–978. <https://doi.org/10.1038/s41893-020-00620-3>.
- 417 Ambrose, J. (2020). Oil prices slump as markets face lowest demand in 25  
418 years. Available at [https://www.theguardian.com/business/2020/apr/15/](https://www.theguardian.com/business/2020/apr/15/oil-prices-slump-as-market-faces-lowest-demand-in-25-years-covid-19)  
419 [oil-prices-slump-as-market-faces-lowest-demand-in-25-years-covid-19](#). The Guardian,  
420 [online; accessed 19-February-2021].
- 421 Arribas-Bel, D., Green, M., Rowe, F., and Singleton, A. (2021). Open data products—a framework for creating valu-  
422 able analysis ready data. *Journal of Geographical Systems*, 23(4):497–514. [https://doi.org/10.1007/](https://doi.org/10.1007/s10109-021-00363-5)  
423 [s10109-021-00363-5](#).
- 424 Arribas-Bel, D., Rowe, F., Chen, M., and Comber, S. (2022). “An image library” The potential of imagery in Regional Science.  
425 In Rey, S. and Franklin, R., editors, *Handbook of Spatial Analysis in the Social Sciences*, pages 1–25. Edward Elgar. in press.
- 426 Aruga, K., Islam, M. M., and Jannat, A. (2020). Effects of COVID-19 on Indian energy consumption. *Sustainability*,  
427 12(14):5616. <https://doi.org/10.3390/su12145616>.
- 428 Bahmanyar, A., Estebarsari, A., and Ernst, D. (2020). The impact of different COVID-19 containment measures on electricity  
429 consumption in Europe. *Energy Research & Social Science*, 68. [https://doi.org/10.1016/j.erss.2020.](https://doi.org/10.1016/j.erss.2020.101683)  
430 [101683](#).
- 431 Baka, J. and Vaishnava, S. (2020). The evolving borderland of energy geographies. *Geography Compass*, 14(7):e12493.  
432 <https://doi.org/10.1111/gec3.12493>.
- 433 Batty, M. (2020). The coronavirus crisis: What will the post-pandemic city look like? *Environment and Planning B: Urban*  
434 *Analytics and City Science*, 47(4):547–552. <https://doi.org/10.1177/2399808320926912>.
- 435 Beyer, R. C., Franco-Bedoya, S., and Galdo, V. (2021). Examining the economic impact of COVID-19 in India through  
436 daily electricity consumption and nighttime light intensity. *World Development*, 140. [https://doi.org/10.1016/j.](https://doi.org/10.1016/j.worlddev.2020.105287)  
437 [worlddev.2020.105287](#).
- 438 Bouzarovski, S. and Thomson, H. (2018). Energy vulnerability in the grain of the city: Toward neighborhood typologies of  
439 material deprivation. *Annals of the American Association of Geographers*, 108(3):695–717. [https://doi.org/10.](https://doi.org/10.1080/24694452.2017.1373624)  
440 [1080/24694452.2017.1373624](#).
- 441 Brosemer, K., Schelly, C., Gagnon, V., Arola, K. L., Pearce, J. M., Bessette, D., and Olabisi, L. S. (2020). The energy crises  
442 revealed by COVID: Intersections of indigeneity, inequity, and health. *Energy Research & Social Science*, 68:101661.  
443 <https://doi.org/10.1016/j.erss.2020.101661>.
- 444 Broto, V. C. and Baker, L. (2018). Spatial adventures in energy studies: An introduction to the special issue. *Energy Research*  
445 *& Social Science*, 36:1–10. <https://doi.org/10.1016/j.erss.2017.11.002>.

- 446 Broto, V. C. and Kirshner, J. (2020). Energy access is needed to maintain health during pandemics. *Nature Energy*, 5:2058–7546.  
447 <https://doi.org/10.1038/s41560-020-0625-6>.
- 448 Brunson, C. and Comber, A. (2021). Opening practice: supporting reproducibility and critical spatial data science. *Journal of*  
449 *Geographical Systems*, 23(4):477–496. <https://doi.org/10.1007/s10109-020-00334-2>.
- 450 Bustamante-Calabria, M., Sánchez de Miguel, A., Martín-Ruiz, S., Ortiz, J.-L., Vílchez, J. M., Pelegrina, A., García, A.,  
451 Zamorano, J., Bennie, J., and Gaston, K. J. (2021). Effects of the COVID-19 lockdown on urban light emissions: Ground  
452 and satellite comparison. *Remote Sensing*, 13:2072–4292. <https://doi.org/10.3390/rs13020258>.
- 453 Cao, C., Xiaoxiong, X., Wolfe, R., DeLuccia, F., Liu, Q. M., Blonski, S., Lin, G. G., Nishihama, M., Pogorzala, D., Oudrari, H.,  
454 and Hillger, D. (2017). NOAA Technical Report NESDIS 142 Visible Infrared Imaging Radiometer Suite (VIIRS) Sensor  
455 Data Record (SDR) User's Guide Version 1.3. *NOAA Technical Report NESDIS 142*, pages 1–40.
- 456 Carvalho, M., de Mello Delgado, D. B., de Lima, K. M., de Camargo Cancela, M., dos Siqueira, C. A., and de Souza, D. L. B.  
457 (2021). Effects of the COVID-19 pandemic on the Brazilian electricity consumption patterns. *International Journal of*  
458 *Energy Research*, 45:3358–3364. <https://doi.org/10.1002/er.5877>.
- 459 Chen, C.-F., de Rubens, G. Z., Xu, X., and Li, J. (2020). Coronavirus comes home? energy use, home energy management, and  
460 the social-psychological factors of COVID-19. *Energy Research & Social Science*, 68:22146296. <https://doi.org/10.1016/j.erss.2020.101688>.
- 461
- 462 Connolly, C., Ali, S. H., and Keil, R. (2020). On the relationships between COVID-19 and extended urbanization. *Dialogues in*  
463 *Human Geography*, 10:2043–8206. <https://doi.org/10.1177/2043820620934209>.
- 464 Dighe, A., Cattarino, L., Cuomo-Dannenburg, G., Skarp, J., Imai, N., Bhatia, S., Gaythorpe, K. A. M., Ainslie, K. E. C.,  
465 Baguelin, M., Bhatt, S., Boonyasiri, A., Brazeau, N. F., Cooper, L. V., Coupland, H., Cucunuba, Z., Dorigatti, I., Eales, O. D.,  
466 van Elsland, S. L., FitzJohn, R. G., Green, W. D., Haw, D. J., Hinsley, W., Knock, E., Laydon, D. J., Mellan, T., Mishra, S.,  
467 Nedjati-Gilani, G., Nouvellet, P., Pons-Salort, M., Thompson, H. A., Unwin, H. J. T., Verity, R., Vollmer, M. A. C., Walters,  
468 C. E., Watson, O. J., Whittaker, C., Whittles, L. K., Ghani, A. C., Donnelly, C. A., Ferguson, N. M., and Riley, S. (2020).  
469 Response to COVID-19 in South Korea and implications for lifting stringent interventions. *BMC Medicine*, 18:1741–7015.  
470 <https://doi.org/10.1186/s12916-020-01791-8>.
- 471 Elvidge, C. D., Baugh, K. E., Zhizhin, M., and Hsu, F.-C. (2013). Why VIIRS data are superior to DMSP for mapping nighttime  
472 lights. *Proceedings of the Asia-Pacific Advanced Network*, 35(0):62. <http://dx.doi.org/10.7125/APAN.35.7>.
- 473 Gebresslassie, M. G. (2020). COVID-19 and energy access: An opportunity or a challenge for the African continent? *Energy*  
474 *Research & Social Science*, 68:22146296. <https://doi.org/10.1016/j.erss.2020.101677>.
- 475 Geels, F. W., Sovacool, B. K., Schwanen, T., and Sorrell, S. (2017). The socio-technical dynamics of low-carbon transitions.  
476 *Joule*, 1:25424351. <https://doi.org/10.1016/j.joule.2017.09.018>.
- 477 Gillingham, K. T., Knittel, C. R., Li, J., Ovaere, M., and Reguant, M. (2020). The Short-run and Long-run Effects of Covid-19  
478 on Energy and the Environment. *Joule*, 4:25424351. <https://doi.org/10.1016/j.joule.2020.06.010>.
- 479 González-Leonardo, M., López-Gay, A., Recaño Valverde, J., and Rowe, F. (2022). Changes of residence in times of COVID-19:  
480 a small respite from rural depopulation. *Perspectives Demographiques*, 26:1–4.
- 481 Google (2020). Google COVID-19 community mobility reports. Available at [https://www.google.com/covid19/](https://www.google.com/covid19/mobility/)  
482 [mobility/](https://www.google.com/covid19/mobility/) (01/07/2021).
- 483 Green, M., Pollock, F. D., and Rowe, F. (2021). New forms of data and new forms of opportunities to monitor and tackle a  
484 pandemic. In "Andrews, G. J., Crooks, V. A., Pearce, J. R., and Messina, J. P., editors, *COVID-19 and Similar Futures*, pages  
485 423–429. Springer. [https://doi.org/10.1007/978-3-030-70179-6\\_56](https://doi.org/10.1007/978-3-030-70179-6_56).
- 486 Hale, T., Angrist, N., Goldszmidt, R., Kira, B., Petherick, A., Phillips, T., Webster, S., Cameron-Blake, E., Hallas, L., Majumdar,  
487 S., and Tatlow, H. (2021). A global panel database of pandemic policies (Oxford COVID-19 Government Response Tracker).  
488 *Nature Human Behaviour*, 5:2397–3374. <https://doi.org/10.1038/s41562-021-01079-8>.
- 489 Hamidi, S., Sabouri, S., and Ewing, R. (2020). Does density aggravate the COVID-19 pandemic? *Journal of the American*  
490 *Planning Association*, 86:0194–4363. <https://doi.org/10.1080/01944363.2020.1777891>.
- 491 Hastie, T., Tibshirani, R., and Friedman, J. (2009). *The Elements of Statistical Learning*. Springer New York. <https://doi.org/10.1007/978-0-387-84858-7>.
- 492
- 493 Henry, M. S., Bazilian, M. D., and Markuson, C. (2020). Just transitions: Histories and futures in a post-COVID world. *Energy*  
494 *Research & Social Science*, 68:22146296. <https://doi.org/10.1016/j.erss.2020.101668>.
- 495 International Energy Agency (2020). The COVID-19 crisis is causing the biggest fall in global energy investment in history.  
496 Technical report, International Energy Agency (IEA).
- 497 International Energy Agency (2021). Global energy review 2021. Technical report, International Energy Agency (IEA).
- 498 International Monetary Fund (2021). World Economic Outlook Update, April 2021. Technical report, International Monetary  
499 Fund (IMF).

- 500 Kanda, W. and Kivimaa, P. (2020). What opportunities could the COVID-19 outbreak offer for sustainability transitions  
501 research on electricity and mobility? *Energy Research & Social Science*, 68:22146296. [https://doi.org/10.1016/  
502 j.erss.2020.101666](https://doi.org/10.1016/j.erss.2020.101666).
- 503 Krarti, M. and Aldubyan, M. (2021). Review analysis of COVID-19 impact on electricity demand for residential buildings.  
504 *Renewable and Sustainable Energy Reviews*, 143:110888. <https://doi.org/10.1016/j.rser.2021.110888>.
- 505 Kuzemko, C., Bradshaw, M., Bridge, G., Goldthau, A., Jewell, J., Overland, I., Scholten, D., de Graaf, T. V., and Westphal,  
506 K. (2020). COVID-19 and the politics of sustainable energy transitions. *Energy Research & Social Science*, 68:22146296.  
507 <https://doi.org/10.1016/j.erss.2020.101685>.
- 508 Levin, N., Kyba, C. C., Zhang, Q., de Miguel, A. S., Román, M. O., Li, X., Portnov, B. A., Molthan, A. L., Jechow, A., Miller,  
509 S. D., et al. (2020). Remote sensing of night lights: A review and an outlook for the future. *Remote Sensing of Environment*,  
510 237:111443. <https://doi.org/10.1038/s41597-020-0510-y>.
- 511 Li, X., Zhou, Y., Zhao, M., and Zhao, X. (2020). A harmonized global nighttime light dataset 1992–2018. *Scientific data*,  
512 7(1):1–9. <https://doi.org/10.1038/s41597-020-0510-y>.
- 513 Liu, Q., Sha, D., Liu, W., Houser, P., Zhang, L., Hou, R., Lan, H., Flynn, C., Lu, M., Hu, T., and Yang, C. (2020). Spatiotemporal  
514 patterns of COVID-19 impact on human activities and environment in mainland China using nighttime light and air quality  
515 data. *Remote Sensing*, 12:2072–4292. <https://doi.org/10.3390/rs12101576>.
- 516 Makoni, M. (2021). Tanzania refuses COVID-19 vaccines. *The Lancet*, 397:01406736. [https://doi.org/10.1016/  
517 S0140-6736\(21\)00362-7](https://doi.org/10.1016/S0140-6736(21)00362-7).
- 518 Memmott, T., Carley, S., Graff, M., and Konisky, D. M. (2021). Sociodemographic disparities in energy insecurity among  
519 low-income households before and during the COVID-19 pandemic. *Nature Energy*, 6:2058–7546. [https://doi.org/  
520 10.1038/s41560-020-00763-9](https://doi.org/10.1038/s41560-020-00763-9).
- 521 Mfinanga, S. G., Mnyambwa, N. P., Minja, D. T., Ntinginya, N. E., Ngadaya, E., Makani, J., and Makubi, A. N.  
522 (2021). Tanzania’s position on the COVID-19 pandemic. *The Lancet*, 397:01406736. [https://doi.org/10.1016/  
523 S0140-6736\(21\)00678-4](https://doi.org/10.1016/S0140-6736(21)00678-4).
- 524 Miller, S., Straka, W., Mills, S., Elvidge, C., Lee, T., Solbrig, J., Walther, A., Heidinger, A., and Weiss, S. (2013). Illuminating  
525 the Capabilities of the Suomi National Polar-Orbiting Partnership (NPP) Visible Infrared Imaging Radiometer Suite (VIIRS)  
526 Day/Night Band. *Remote Sensing*, 5. <https://doi.org/10.3390/rs5126717>.
- 527 Min, B., Gaba, K. M., Sarr, O. F., and Agalassou, A. (2013). Detection of rural electrification in Africa using DMSP-OLS night  
528 lights imagery. *International journal of remote sensing*, 34(22):8118–8141. [https://doi.org/10.1080/01431161.  
529 2013.833358](https://doi.org/10.1080/01431161.2013.833358).
- 530 Mohammadi, N. and Taylor, J. E. (2017). Urban energy flux: Spatiotemporal fluctuations of building energy consumption and  
531 human mobility-driven prediction. *Applied Energy*, 195. [https://doi.org/10.1016/j.apenergy.2017.03.  
532 044](https://doi.org/10.1016/j.apenergy.2017.03.044).
- 533 Munayco, C. V., Tariq, A., Rothenberg, R., Soto-Cabezas, G. G., Reyes, M. F., Valle, A., Rojas-Mezarina, L., Cabezas, C.,  
534 Loayza, M., Chowell, G., et al. (2020). Early transmission dynamics of COVID-19 in a southern hemisphere setting:  
535 Lima-Peru: February 29th–March 30th, 2020. *Infectious Disease Modelling*, 5:338–345. [https://doi.org/10.  
536 1016/j.idm.2020.05.001](https://doi.org/10.1016/j.idm.2020.05.001).
- 537 Norouzi, N., de Rubens, G. Z., Choupanpiesheh, S., and Enevoldsen, P. (2020). When pandemics impact economies and climate  
538 change: Exploring the impacts of COVID-19 on oil and electricity demand in China. *Energy Research & Social Science*,  
539 68:22146296. <https://doi.org/10.1016/j.erss.2020.101654>.
- 540 Phillips, N. (2021). The coronavirus is here to stay — here’s what that means. *Nature*, 590.
- 541 Pinghui, J. and Ma, Z. (2020). 5 million left wuhan before lockdown, 1,000 new coronavirus cases expected in city.
- 542 Qarnain, S. S., Sattanathan, M., Sankaranarayanan, B., and Ali, S. M. (2020). Analyzing energy consumption factors during  
543 coronavirus (COVID-19) pandemic outbreak: a case study of residential society. *Energy sources, part a: Recovery, utilization,  
544 and environmental effects*, pages 1–20. <https://doi.org/10.1080/15567036.2020.1859651>.
- 545 Ritchie, H., Mathieu, E., Rodés-Guirao, L., Appel, C., Giattino, C., Ortiz-Ospina, E., Hasell, J., Macdonald, B., Beltekian, D.,  
546 and Roser, M. (2020). Coronavirus pandemic (COVID-19). *Our World in Data*. [https://ourworldindata.org/  
547 coronavirus](https://ourworldindata.org/coronavirus).
- 548 Robinson, C., Lindley, S., and Bouzarovski, S. (2019). The spatially varying components of vulnerability to energy poverty.  
549 *Annals of the American Association of Geographers*, 109(4):1188–1207. [https://doi.org/10.1080/24694452.  
550 2018.1562872](https://doi.org/10.1080/24694452.2018.1562872).
- 551 Román, M. O., Stokes, E. C., Shrestha, R., Wang, Z., Schultz, L., Carlo, E. A. S., Sun, Q., Bell, J., Molthan, A., Kalb, V.,  
552 et al. (2019). Satellite-based assessment of electricity restoration efforts in Puerto Rico after Hurricane Maria. *PLoS one*,  
553 14(6):e0218883. <https://doi.org/10.1371/journal.pone.0218883>.

554 Rowe, F., Calafiore, A., Arribas-Bel, D., Samardzhiev, K., and Fleischman, M. (2022). Understanding the Patterns of Human  
555 Mobility in Britain During the COVID-19 Pandemic Using Facebook Data. *preprint*, pages 1–17.

556 Ruan, G., Wu, D., Zheng, X., Zhong, H., Kang, C., Dahleh, M. A., Sivaranjani, S., and Xie, L. (2020). A cross-domain  
557 approach to analyzing the short-run impact of COVID-19 on the US electricity sector. *Joule*, 4:25424351. <https://doi.org/10.1016/j.joule.2020.08.017>.

558

559 Schiavina, M., Moreno-Monroy, A., Maffeni, L., and Veneri, P. (2019). GHSL-OECD Functional Urban Areas. Technical  
560 report, Publications Office of the European Union.

561 Schot, J., Kanger, L., and Verbong, G. (2016). The roles of users in shaping transitions to new energy systems. *Nature Energy*,  
562 1:2058–7546. <https://doi.org/10.1038/nenergy.2016.54>.

563 Stevens, F. R., Gaughan, A. E., Linard, C., and Tatem, A. J. (2015). Disaggregating census data for population mapping using  
564 random forests with remotely-sensed and ancillary data. *PLOS ONE*, 10:1932–6203. [https://doi.org/10.1371/](https://doi.org/10.1371/journal.pone.0107042)  
565 [journal.pone.0107042](https://doi.org/10.1371/journal.pone.0107042).

566 United Nations (2018). Work urbanization prospects 2018: Highlights. Technical report, United Nations.

567 Wang, Z., Román, M., Sun, Q., Molthan, A., Schultz, L., and Kalb, V. (2018). Monitoring disaster-related power outages using  
568 NASA black marble nighttime light product. *ISPRS Int. Arch. Photogramm. Remote Sens. Spat. Inf. Sci.*, pages 1853–1856.

569 Watanabe, T. and Yabu, T. (2021). Japan’s voluntary lockdown. *PLOS ONE*, 16:1932–6203. [https://doi.org/10.](https://doi.org/10.1371/journal.pone.0252468)  
570 [1371/journal.pone.0252468](https://doi.org/10.1371/journal.pone.0252468).

571 Werth, A., Gravino, P., and Prevedello, G. (2021). Impact analysis of COVID-19 responses on energy grid dynamics in Europe.  
572 *Applied Energy*, 281:116045. <https://doi.org/10.1016/j.apenergy.2020.116045>.

573 Xu, G., Xiu, T., Li, X., Liang, X., and Jiao, L. (2021). Lockdown induced night-time light dynamics during the COVID-19  
574 epidemic in global megacities. *International Journal of Applied Earth Observation and Geoinformation*, 102:03032434.  
575 <https://doi.org/10.1016/j.jag.2021.102421>.

576 Zheng, B., Geng, G., Ciais, P., Davis, S. J., Martin, R. V., Meng, J., Wu, N., Chevallier, F., Broquet, G., Boersma, F., van der A,  
577 R., Lin, J., Guan, D., Lei, Y., He, K., and Zhang, Q. (2020). Satellite-based estimates of decline and rebound in China’s CO2  
578 emissions during COVID-19 pandemic. *Science Advances*, 6:2375–2548. [https://doi.org/10.1126/sciadv.](https://doi.org/10.1126/sciadv.abd4998)  
579 [abd4998](https://doi.org/10.1126/sciadv.abd4998).

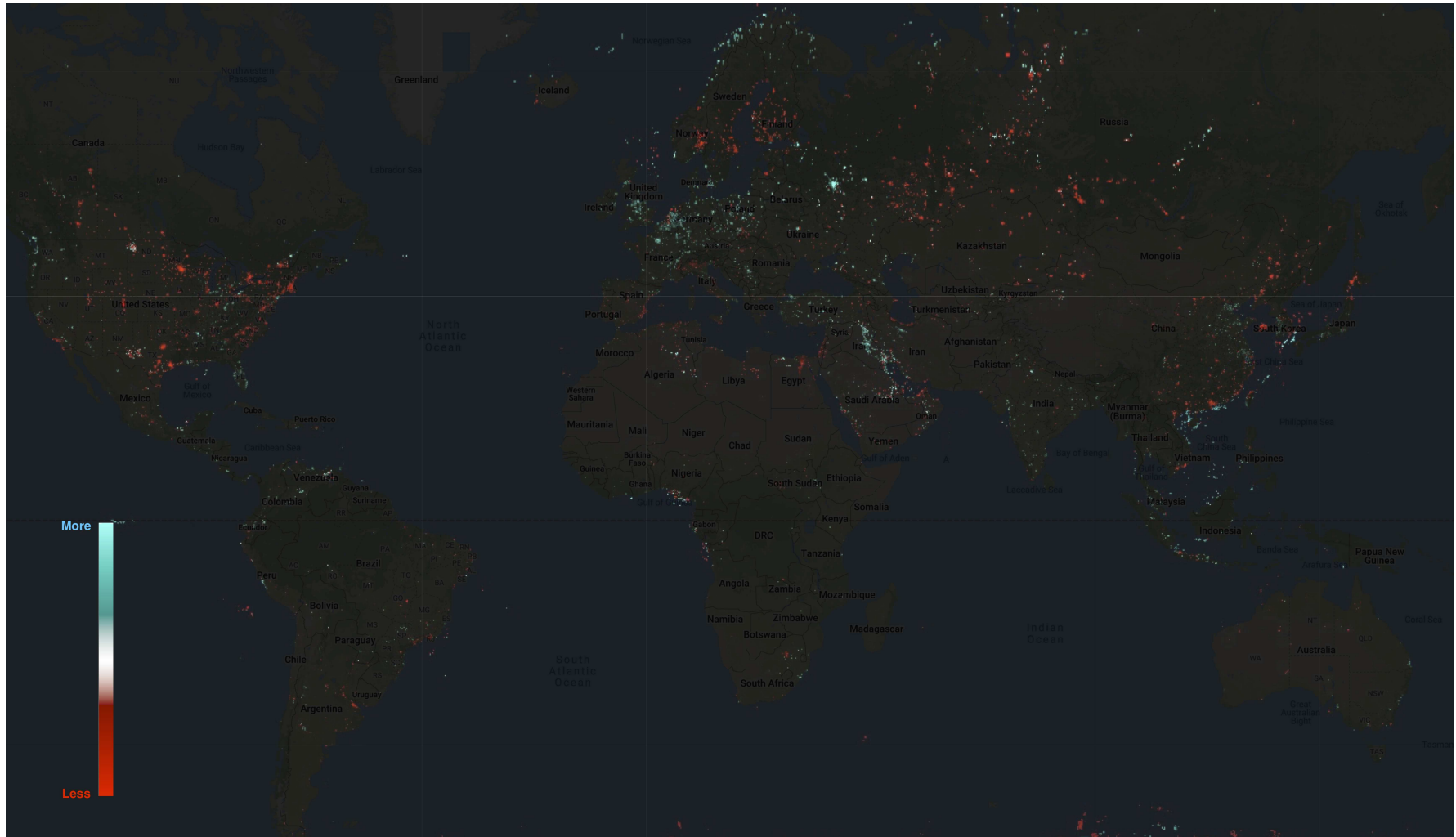


**Figure 1. Global map of NTL intensity.** Difference in radiance between December 2019 and March 2020. Red encodes a reduction in NTL intensity (i.e. dimmed). Blue encodes an increase (i.e. brightened). NTL imagery was extracted from the Payne Institute for Public Policy (<https://payneinstitute.mines.edu/eog/nighttime-lights/>).

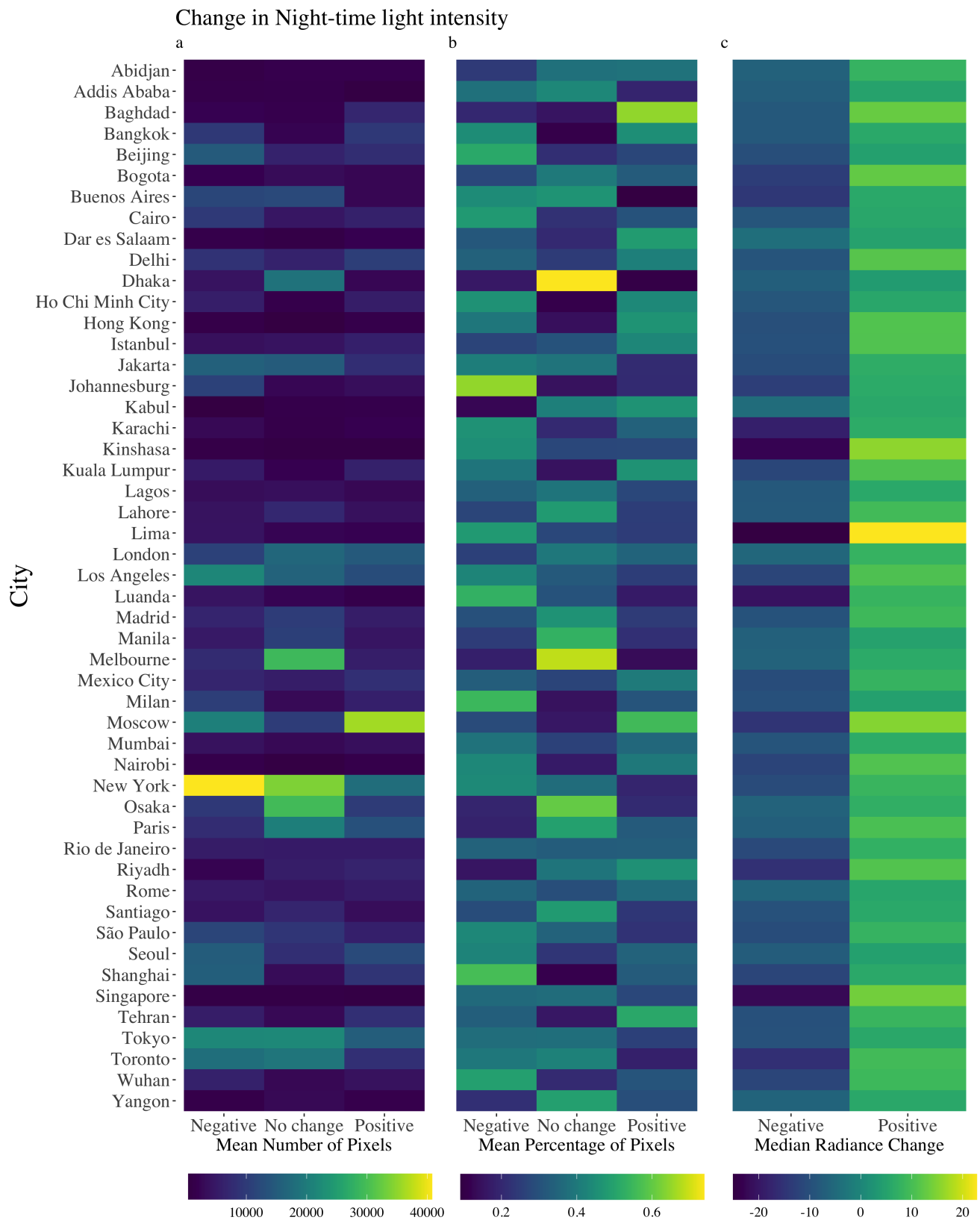


**Figure 2. Indicators of changes in NTL intensity.** **a** Mean number of pixels: Average number of changing pixels. **b** Mean percentage of pixels. **c** Median radiance change: Median radiance of NTL intensity. These indicators refer to the difference between individual months (January 2020, February 2020, March 2020, April 2020, May 2020, and June 2020) and December 2019 across three categories: negative, neutral and positive. NTL imagery was extracted from the Payne Institute for Public Policy (<https://payneinstitute.mines.edu/eog/nighttime-lights/>).

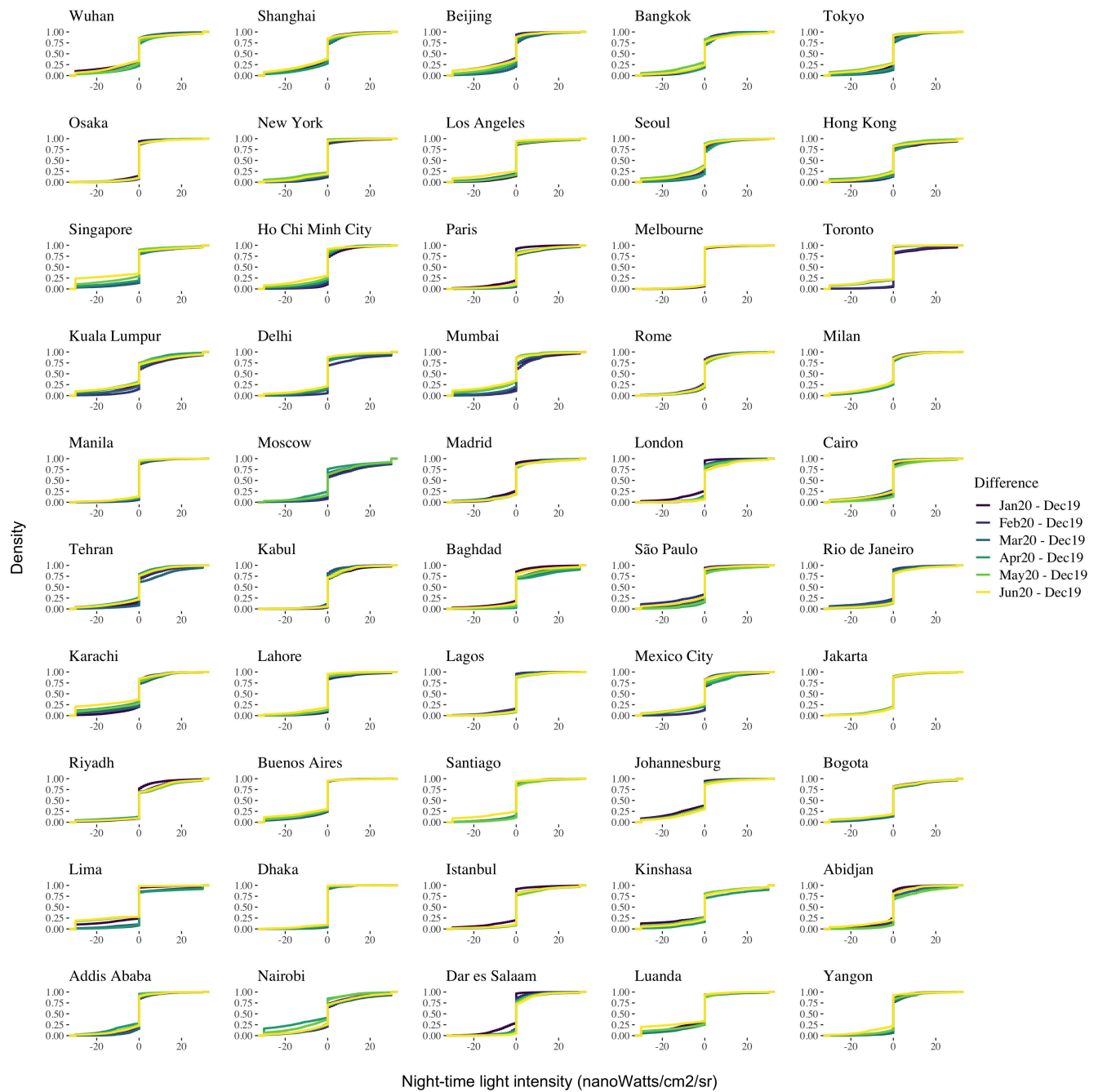


**Figure 3. Change in NTL intensity.** Each line in the graph represents the difference in NTL intensity between each individual month (January 2020, February 2020, March 2020, April 2020, May 2020 and June 2020) and our baseline month (December 2019). The y-axis indicates the proportion of pixels at each value of the difference in night-time light intensity between relevant months. Comparing across density distributions provides an indication of the magnitude of change in night-time light intensity over time. NTL imagery was extracted from the Payne Institute for Public Policy (<https://payneinstitute.mines.edu/eog/nighttime-lights/>)

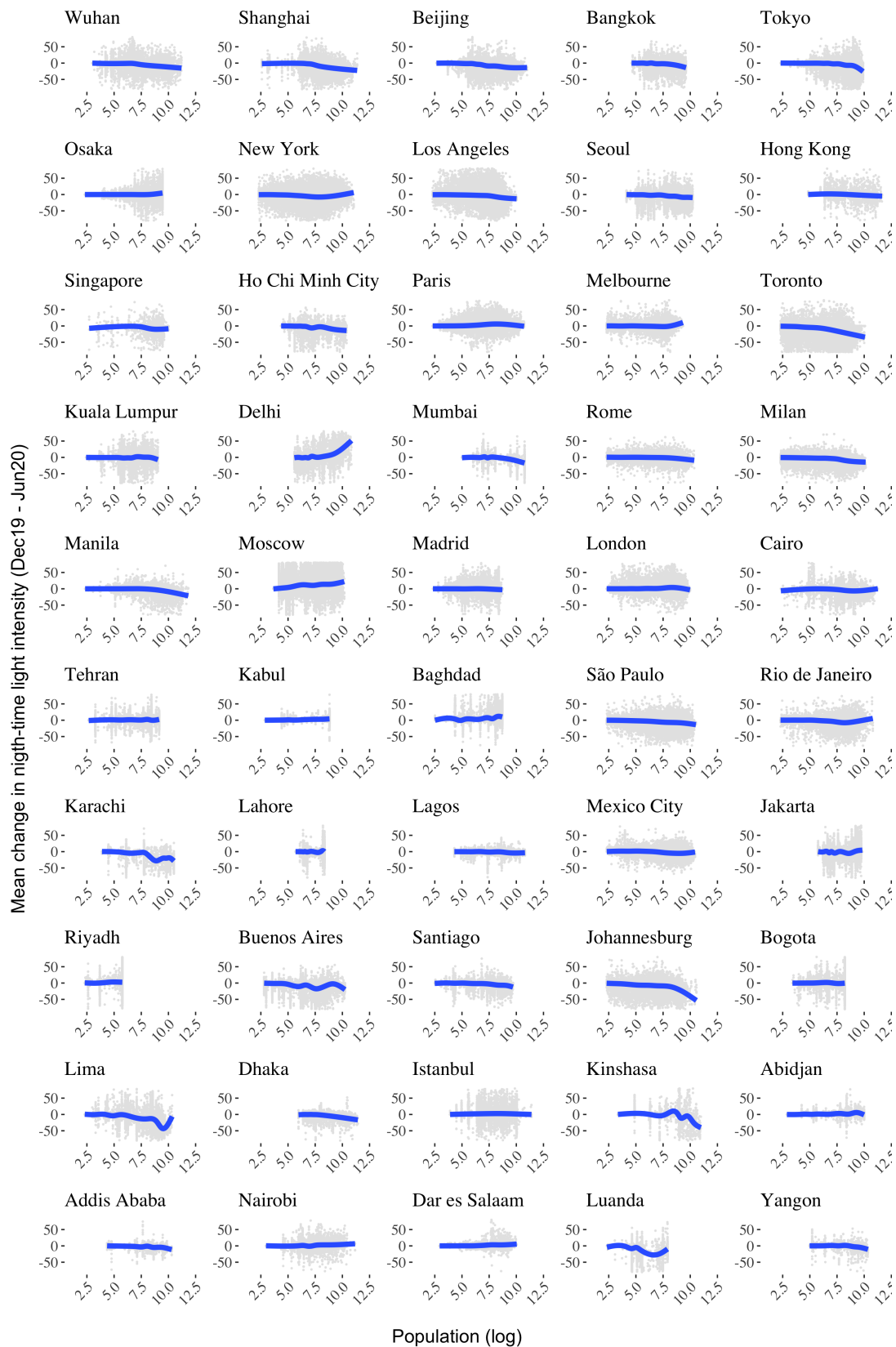


**Figure 4. Relationship between population density (log) and average change in NTL intensity.** The average in NTL intensity corresponds to the difference across individual months (January - June 2020) and December 2019 (baseline). NTL imagery was extracted from the Payne Institute for Public Policy (<https://payneinstitute.mines.edu/eog/nighttime-lights/>). Population density data were obtained from the WordPop project (<https://www.worldpop.org> - see Stevens et al., 2015).

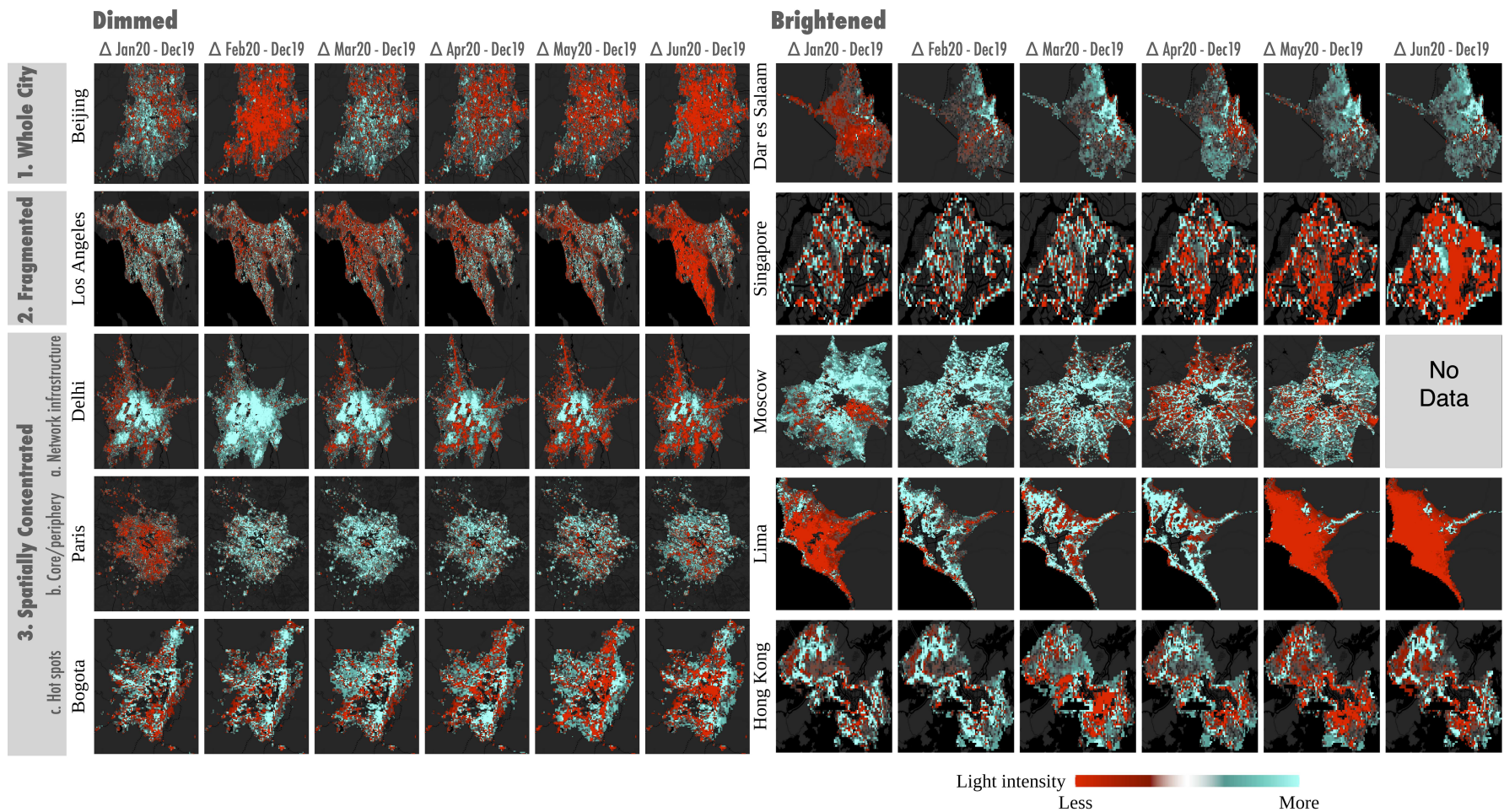


**Figure 5. Classification of global cities according to change in NTL intensity.** Pixels shaded in red record a reduction NTL intensity (i.e. dimmed), whilst those shaded in blue record an increase (i.e. brightened). Areas that did not experience a change are not shaded. Interpretation of the imagery in the text is based on the month that national lockdown was first imposed in each city (SM Table 2). Where the date of lockdown was close to the end of the month, imagery for the following month was used. NTL imagery was extracted from the Payne Institute for Public Policy (<https://payneinstitute.mines.edu/eog/nighttime-lights/>).

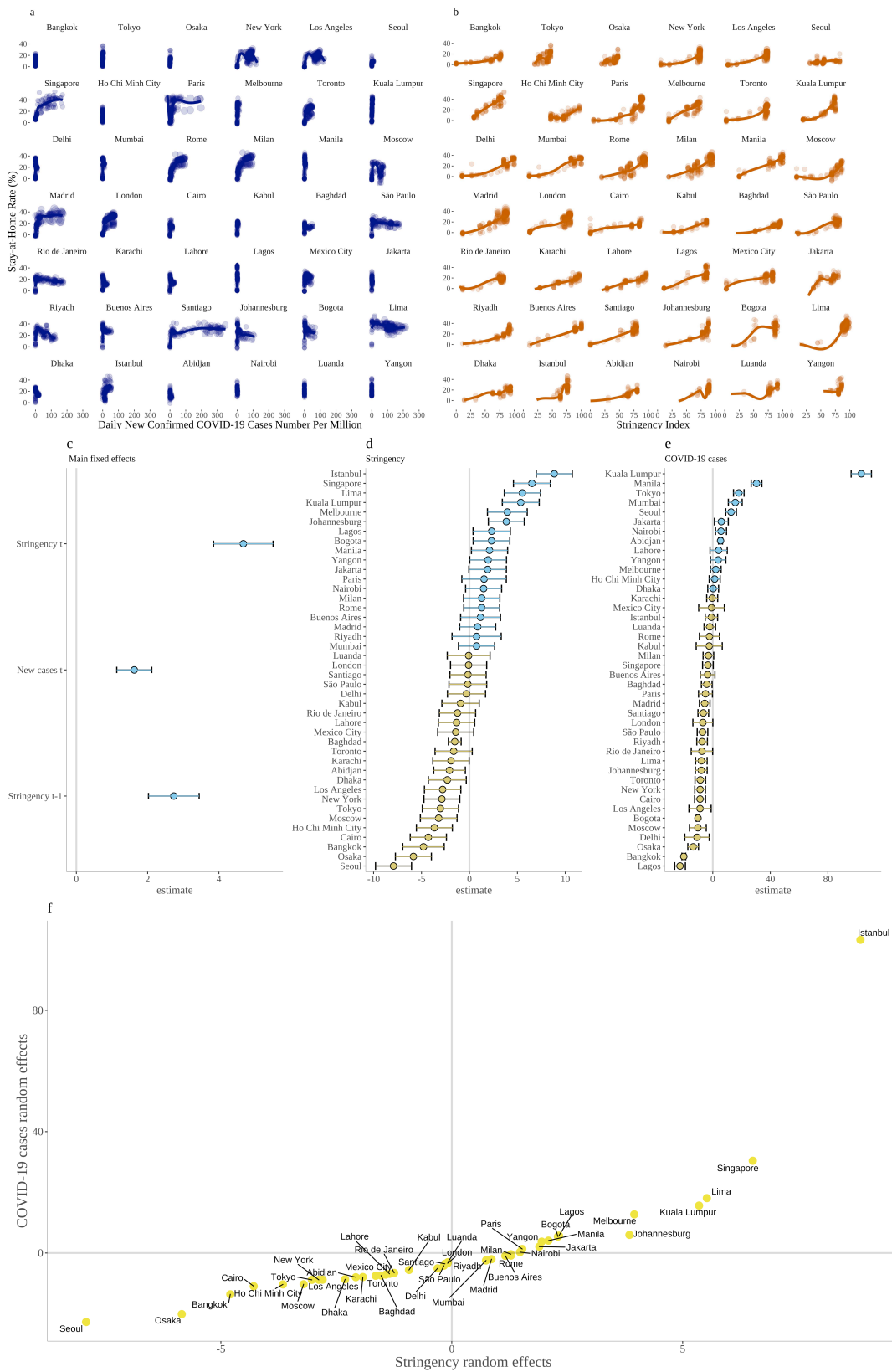


**Figure 6. Association between stay-at-home population, stringency and COVID-19 cases. a** Relationship between stay-at-home population and new COVID-19 cases per million. **b** Relationship between stay-at-home population and stringency index. **c** Regression coefficients: main fixed effects were obtained from Equation 4. **d** Regression coefficients: random effects for stringency across cities were obtained from Equation 5. **e** Regression coefficients: random effects for COVID-19 cases across cities were obtained from Equation 6. **f** Classification based on stringency and COVID-19 cases random effects estimated via Equation 5 and 6.

## Supplementary Files

This is a list of supplementary files associated with this preprint. Click to download.

- [nepapersm.pdf](#)